

# A Mobile NMR System with Full Spectroscopy Capability

Chao Ma and Zhi-Pei Liang

**Abstract**—This paper reports our work in developing a mobile nuclear magnetic resonance system with full spectroscopy capability. The system consists of a 0.93 T, portable permanent magnet, a 8-turn 550  $\mu\text{m}$  diameter microcoil, and compact electronics systems. The system provides 0.4 parts per million spectrum linewidth and 408 signal-to-noise ratio from a 37 nL water sample with 128 averages. Representative  $^1\text{H}$  and  $^{19}\text{F}$  spectra are presented.

## I. INTRODUCTION

Nuclear magnetic resonance (NMR) is a unique physical phenomenon, which has been widely used for studying chemical structure of materials and for non-destructive analyte identification and quantification. However, conventional NMR systems are designed and built for applications requiring high signal-to-noise ratio (SNR) and spectral resolution using strong superconducting magnets. Developing mobile NMR systems will enable new NMR applications that are difficult to perform using conventional NMR systems, such as on-site detection of toxic materials in environmental sensing, detection of bacteria/biomarkers for point-of-care diagnosis, and large-scale, parallel NMR analysis of biochemical samples for drug discovery.

In the past decade, significant technology advances in portable magnets, NMR coils and NMR electronics have been made to tackle the SNR and spectral resolution challenges while scaling down conventional NMR systems to portable sizes. Continuous efforts have been made to design portable permanent magnets of higher field strength and better homogeneity [1], [2], [3]. NMR microcoil techniques [4], [5] (*e.g.*, coils much smaller than 5 mm diameter) have dramatically increased the detection sensitivity of NMR (*i.e.*, the minimum detectable volume of samples), which is critical toward a mobile NMR system since portable magnets usually provide sufficient homogeneity only in a volume-limited region (*e.g.*, a 0.5 mm diameter sphere). It has been demonstrated that NMR spectra can be successfully collected using microcoils and portable magnets at field strength of 0.7  $\sim$  2 T [2], [6], [7], [8]. The narrowest linewidth reported is around 0.2 parts per million (ppm) [2], [3]. However, these prototype systems are built with commercial NMR electronics designed for conventional NMR systems, which are bulky for mobile applications and not specially optimized for mobile NMR systems. More recently, truly portable NMR systems with integrated microcoil and microfluidics chips

and compact NMR electronics have been developed and shown exciting results in bacteria/cancer cells detection and biomarker analysis using magnetic nanoparticle biosensors [9], [10], [11]. Furthermore, radio frequency (RF) integrated circuits (ICs) have been developed to integrate NMR electronics into IC chips [12], [13]. However, the systems in [9], [10], [11] have limited NMR capabilities, *i.e.*, only relaxation parameters rather than NMR spectra are measured.

This paper presents our work in developing a mobile NMR system with full NMR spectroscopy capability. The prototype system consists of: a) a portable permanent magnet that has 0.93 T field strength and weights about 1 pound; b) a solenoidal microcoil of 550  $\mu\text{m}$  diameter on a glass capillary; c) compact NMR electronics; and d) signal processing software especially for data averaging.  $^1\text{H}$  spectra of 0.4 ppm linewidth and 408 SNR over 128 averages from a 37 nL water sample have been achieved. In preparing this paper, we note that a commercial mobile NMR system of full spectroscopy capability has been recently released [14].

The rest of the paper is organized as follows: Section II describes the design of the mobile NMR system in detail; Section III presents representative  $^1\text{H}$  and  $^{19}\text{F}$  spectra collected using the mobile system; Section IV contains the conclusions of the paper.

## II. MOBILE NMR SYSTEM

The mobile NMR system in this work consists of a portable permanent magnet for spin polarization, a microcoil for NMR signal excitation and detection, compact electronics system for NMR pulse generation and NMR signal acquisition, and signal processing software. In the following, the design requirements and implementation details of each component are described.

### A. Portable permanent magnet

The primary requirements of the magnet of a mobile NMR system are strong magnetic field strength (for high SNR), good field homogeneity (for high spectral resolution) and portability. The magnet of our system is essentially the same type of magnet used in [2], which provides, so far, the best tradeoff among magnetic field strength, spectral resolution, and magnet weight in commercially available permanent magnets [2]. More specifically, the magnet (shown in Fig. 1a) is a 0.93 T, Samarium Cobalt permanent magnet (Aster Enterprises, Acton, MA), and weights about 1 pound. The magnet was designed to provide 10 ppm homogeneity over a 0.5 mm diameter sphere volume.

\*This work was supported by a Beckman graduate fellowship (Chao Ma). Chao Ma and Zhi-Pei Liang are with the Department of Electrical and Computer Engineering and Beckman Institute for Advanced Science and Technology, University of Illinois at Urbana-Champaign, 1406 West Green Street, Urbana, IL 61801. chaoma2,z-liang@illinois.edu

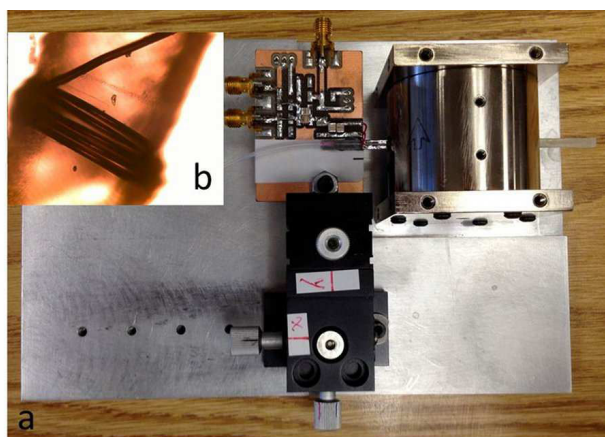


Fig. 1. **a:** The magnet, stage, and matching and tuning circuit of the mobile NMR system. **b:** Microscopy image of a 5-turn microcoil.

### B. Microcoil

In a mobile NMR system, the samples are often constrained to a very small region of the portable magnet that can provide good homogeneity for sufficient NMR spectral resolution. Microcoil techniques that can significantly increase the coil detection sensitivity for volume-limited samples [4], [5] is a critical component of a mobile NMR system. More specifically, the detection sensitivity of a solenoidal coil (in the term of SNR per unit volume sample) is inverse proportional to the diameter of the coil:

$$\frac{SNR}{\nu_s} \propto \frac{\omega_0^{7/4}}{d}, \quad (1)$$

where  $\nu_s$  is the sample volume,  $\omega_0$  is the resonance frequency (rad/s),  $d$  is the diameter of the coil, and the number of turns and length/diameter ratio of the solenoidal coils are assumed to be fixed. According to Eq. (1), a microcoil of 500  $\mu\text{m}$  diameter will increase the detection sensitivity by 10 times compared with a conventional 5 mm diameter coil, which means 100 times experiment time reduction if averaging is used to improve the detection sensitivity!

The microcoils in our system were hand-wound around 550  $\mu\text{m}$  o.d. and 400  $\mu\text{m}$  i.d. glass capillaries (Vitrocom, Mountain Lakes, NJ) using 50 gauge enameled copper wire. The wound microcoil was fixed on the capillary using epoxy (Loctite, super glue). Fig. 1b shows the microscopy image of a 5-turn microcoil. An 8-turn microcoil with about 37 nL sample volume was used. The 8-turn microcoil was mounted on a PCB board, which was further mounted on a XYZ translation stage (DT12XYZ, Thorlabs, Newton, NJ) as shown in Fig. 1a.

The resistance and inductance of the 8-turn microcoil was 0.9  $\Omega$  and 54.2 nH measured at 39.7 MHz (resonance frequency of  $^1\text{H}$  at 0.93 T) using a network analyzer (E8357A, Agilent, Santa Clara, CA), which has good agreement with results in [15]. The lead on the mounting PCB board contributed additional 0.3  $\Omega$  resistance and 42.8 nH inductance.

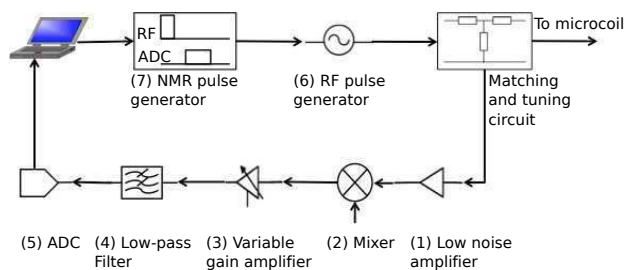


Fig. 2. Electronics system diagram. Brief information of each component is listed in Table I.

### C. Electronics system

The electronics system of the mobile NMR system (shown in Fig. 2) consists of three major components: a) an RF transceiver for NMR signal excitation and detection, b) an NMR pulse generator, and c) a software system that provides interface to control NMR experiments on a PC.

The RF receiver (components (1) - (5) in Fig. 2) is a single conversion digital receiver. The input NMR signal is first amplified by a low noise amplifier, then mixed to an intermediate frequency (*i.e.*, 1.1 MHz IF), further amplified and low-pass filtered. Finally, the IF signal is digitized. Phase sensitive detection is performed in digital domain.

The RF transmitter is simply a digital synthesizer (component (6) in Fig. 2) that provides precise control of the frequency, phase and amplitude of the output RF waveform. An NMR pulse generator that is essentially a digital I/O (component (7) in Fig. 2) is used to program the digital synthesizer to generate RF pulses for NMR signal excitation. Note that the microcoil not only significantly increases the detection sensitivity but also reduces the power for driving RF pulse by several orders of magnitude [6], [15]. For the microcoil in our system, RF power of only tens of microwatts was needed to drive a 100  $\mu\text{s}$  90° RF pulse, which eliminated the need of an RF power amplifier.

Table I summarizes the information of each hardware component of the electronics system. The software system was developed using LabVIEW (National Instruments, Austin, TX).

### D. Signal processing

Once raw data acquired, signal processing is required to perform various tasks, such as phase sensitive detection, downsampling, averaging, denoising, quantification and so on. Data averaging is particularly challenging for a mobile NMR system because of the field drift of a permanent magnet. The field strength of a permanent magnetic is very sensitive to the environment temperature fluctuations. For instance, the permanent magnet of the presented system has a temperature coefficient of -300 K/ppm. Field drift of several Herzs per second is common, which allows only a few averages without significantly broadening the linewidth of the spectrum. One approach to the problem is to build a temperature control system, which, however, could lead to a costly and bulky device. Alternatively, since the field drift only changes the position of the spectrum, and does

TABLE I

BRIEF INFORMATION OF COMPONENTS OF THE ELECTRONICS SYSTEM

No.	Model and Function
(1)	AD8331 low noise amplifier (Analog Devices, Norwood, MA), providing 34 dB gain with 2.5 dB noise figure.
(2)	ZMF-11-S+ mixer (Mini-Circuits, Brooklyn, NY), mixing NMR signals to 1.1 MHz IF.
(3)	AD8330 variable gain amplifier (Analog Devices), providing another 32 dB gain.
(4)	BLP-1.9+ low pass filter (Mini-Circuits), filtering IF signals with 1.9 MHz passband cutoff frequency.
(5)	CS8240 digitizer (Gage Applied Technologies, Lockport, IL), digitizing NMR signals at 5 MS/s with 12-bit resolution.
(6)	AD9854 digital synthesizer (Analog Devices), generating RF signals with 48-bit frequency resolution, 14-bit phase resolution and 12-bit amplitude resolution.
(7)	NI PCIe-6535 10 MHz digital I/O (National Instruments, Austin, TX), generating NMR pulses.

not affect the shape of the spectrum (that is determined by chemical shift, coupling and relaxation), averaging can be done if the measured spectra are aligned properly through post-processing.

In our system, averaging was performed using the second approach. First, wide-bandwidth RF hard pulses (100  $\mu$ s, 12.1 kHz bandwidth) were used to make sure spins were excited during the experiments in the presence of field drifts. Second, the NMR spectrum of the  $i$ -th ( $i > 1$ ) experiment ( $s_i(n)$ ) was aligned to that of the first experiment ( $s_1(n)$ ) by:

$$s_{i,\text{aligned}}(n) = s_i(n)e^{-j(\omega_i^* n\Delta t + \theta_i^*)}, \quad (2)$$

$$[\omega_i^*, \theta_i^*] = \arg \min_{\omega_i, \theta_i} \sum_{n=1}^N \|s_i(n)e^{-j(\omega_i n\Delta t + \theta_i)} - s_1(n)\|^2, \quad (3)$$

where  $\omega_i^*$  is the frequency shift of the  $i$ -th experiment,  $\theta_i^*$  is the phase change,  $\Delta t$  is the sampling period, and  $s_{i,\text{aligned}}(n)$  is the aligned time-domain NMR signals of the  $i$ -th experiment. All the signal processing algorithms including phase sensitive detection, downsampling, averaging and fitting were implemented using MATLAB (MathWorks, Natick, MA).

### III. RESULTS

The microcoil was first tuned to the resonance frequency of proton (39.7 MHz at 0.93 T) to collect  $^1\text{H}$  spectra. The position of the microcoil was carefully adjusted using the XYZ stage to optimize the spectrum linewidth. Fig. 3 shows the free induced decay (FID) signal and its Fourier spectrum (absorption mode after phase correction) collected using our system from a 37 nL water sample with 128 averages. The FID signal was further fitted based on a single decay model. The  $T_2^*$  constant was estimated to be 18.3 ms. The linewidth of the spectrum was estimated to be 0.4 ppm. With 128 averages, the SNR of the FID signal (defined as the ratio of peak signal to noise) and SNR of the NMR spectrum (defined as the ratio of peak spectrum to noise) were 208 and

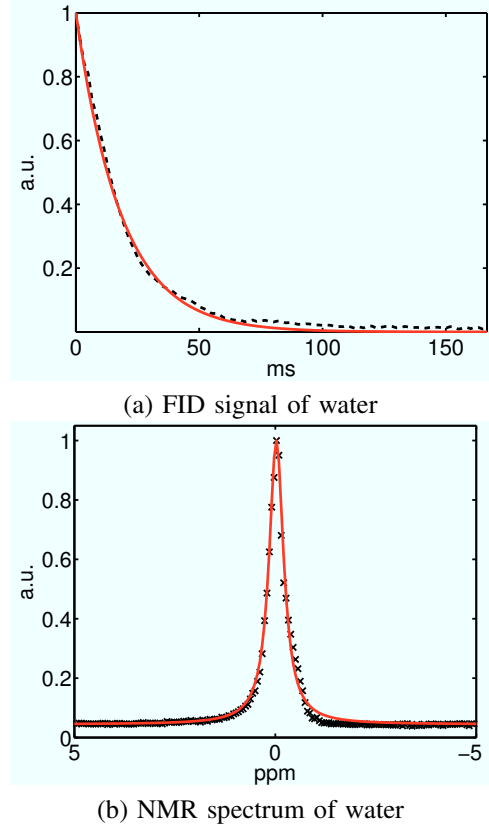


Fig. 3.  $^1\text{H}$  NMR signals from water with 128 averages. **a**: FID signal (black dashed line: measured FID signal; red solid line: fit based on a single decay model). **b**: NMR spectrum, absorption mode (black cross: measured spectrum; red solid line: fit based on a single decay model).

408, respectively. The linewidth could be further reduced if smaller microcoils are used.

Fig. 4 shows the  $^1\text{H}$  NMR spectrum (magnitude plot, unreferenced) of Ethanol ( $\text{CH}_3\text{-CH}_2\text{-OH}$ ). The distance between the  $\text{CH}_3$  peak and the  $\text{CH}_2$  peak was 2.53 ppm that matched well with the prediction (2.47 ppm). The distance between the  $\text{CH}_3$  peak and the  $\text{OH}$  peak was 4.49 ppm. The NMR spectrum was fitted using a single decay model, from which the ratio of the concentrations of the  $^1\text{H}$  atoms in  $\text{CH}_3$ ,  $\text{CH}_2$  and  $\text{OH}$  was estimated to be 2.8:1.9:1.0 that also matched well with the prediction (3:2:1).

The microcoil was also tuned to the resonance frequency of fluorine (37.4 MHz at 0.93 T) to collect  $^{19}\text{F}$  spectra. Fig. 5 shows the NMR spectrum (magnitude plot, unreferenced) of FC-43 ( $(\text{CF}_3\text{-CF}_2\text{-CF}_2\text{-CF}_2)_3\text{N}$ , Fluorinert electronic liquid, 3M, St. Paul, MN). The positions of the three  $\text{CF}_2$  peaks (referred to the  $\text{CF}_3$  peak) were 2.1 ppm, 36.7 ppm and 45.1 ppm, respectively, which also matched well with the prediction (2.0 ppm, 36.4 ppm and 45.1 ppm).

### IV. CONCLUSIONS

In this work, a mobile NMR system with full spectroscopy capability is presented. The system consists of a portable permanent magnet, a solenoidal microcoil, and compact NMR electronics systems. The system provides 0.4 parts per million (ppm) spectrum linewidth and 408 SNR from a 37 nL

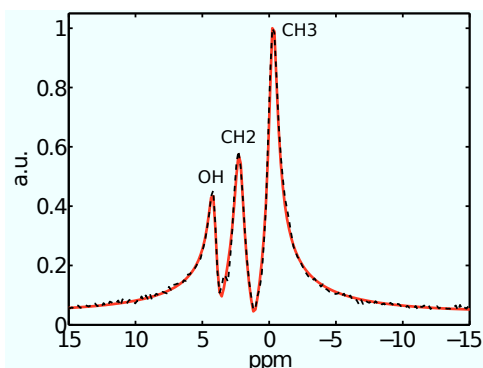


Fig. 4.  $^1\text{H}$  NMR spectrum (magnitude plot) from Ethanol ( $\text{CH}_3\text{-CH}_2\text{-OH}$ ) with 128 averages (black dashed line: measured NMR spectrum; red solid line: fit based on a single decay model).

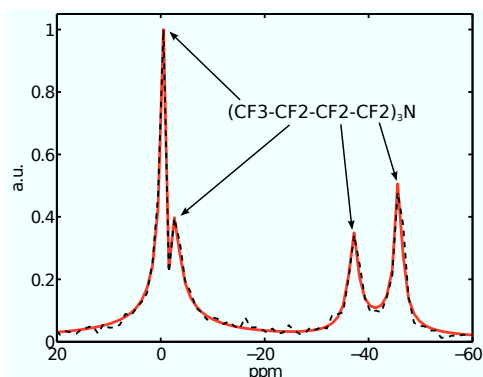


Fig. 5.  $^{19}\text{F}$  NMR spectrum (magnitude plot) from FC-43 ( $(\text{CF}_3\text{-CF}_2\text{-CF}_2\text{-CF}_2)_3\text{N}$ ) with 128 averages (black dashed line: measured NMR spectrum; red solid line: fit based on a single decay model).

water sample with 128 averages. Proton and fluorine NMR spectra have been successfully collected using the system.

#### REFERENCES

- [1] J. Perlo, F. Casanova, and B. Blümich, "Ex situ NMR in highly homogeneous fields:  $^1\text{H}$  spectroscopy," *Science*, vol. 315, pp. 1110-1112, Feb. 2007.
- [2] A. McDowell and E. Fukushima, "Ultracompact NMR:  $^1\text{H}$  spectroscopy in a subkilogram magnet," *Appl. Magn. Reson.*, vol. 35, pp. 185-195, 2008.
- [3] E. Danieli, J. Perlo, B. Blümich and F. Casanova, "Small magnets for portable NMR spectrometers," *Angew. Chem. Int. Ed.*, vol. 49, pp. 4133-4135, 2010.
- [4] T. Peck, R. Magin and P. Lauterbur, "Design and analysis of microcoils for NMR microscopy," *J. Magn. Reson. Series B*, vol. 108, pp. 114-124, 1995.
- [5] D. Olson, T. Peck, A. Webb, R. Magin and J. Sweedler, "High-resolution microcoil  $^1\text{H}$ -NMR for mass-limited, nanoliter-volume samples," *Science*, vol. 270, pp. 1967-1970, Dec. 1995.
- [6] V. Demas, J. Herberg, V. Malba, A. Bernhardt, L. Evans, C. Harvey, S. Chinn, R. Maxwell and J. Reimer, "Portable, low-cost NMR with laser-lathe lithography produced microcoils," *J. Magn. Reson.*, vol. 189, pp. 121-129, 2007.
- [7] S. Küster, E. Danieli, B. Blümich and F. Casanova, "High-resolution NMR spectroscopy under fume hood," *Phys. Chem. Chem. Phys.*, vol. 13, pp. 13172-13176, 2011.
- [8] J. Diekmann, K. Adams, G. Klunder, L. Evans, P. Steele, C. Vogt, and J. Herberg, "Portable microcoil NMR detection coupled to capillary electrophoresis," *Anal. Chem.*, vol. 83, pp. 1328-1335, 2011.
- [9] H. Lee, E. Sun, D. Ham and R. Weissleder, "Chip-NMR biosensor for detection and molecular analysis of cells," *Nature Medicine*, vol. 14, pp. 869-874, Aug. 2008.

- [10] H. Lee, T. Yoon, and R. Weissleder, "Ultrasensitive detection of bacteria using core-shell nanoparticles and an NMR-filter system," *Angew. Chem. Int. Ed.*, vol. 48, pp. 5657-5660, 2009.
- [11] H. Lee, T. Yoon, J. Figueiredo, F. Swirski and R. Weissleder, "Rapid detection and profiling of cancer cells in fine-needle aspirates," *PNAS*, vol. 106, pp. 12459-12464, July 2009.
- [12] N. Sun, Y. Liu, H. Lee, R. Weissleder and D. Ham, "CMOS RF biosensor utilizing nuclear magnetic resonance," *IEEE J. Solid-State Circuits*, vol. 44, pp. 1629-1643, May 2009.
- [13] N. Sun, T. Yoon, H. Lee, W. Andress, W. Demas, P. Prado, R. Weissleder and D. Ham, "Palm NMR and 1-chip NMR," *IEEE J. Solid-State Circuits*, vol. 46, pp. 342-352, Jan. 2011.
- [14] <http://www.picospin.com/>.
- [15] A. McDowell and N. Adolphi, "Operating nanoliter scale NMR microcoils in a 1 tesla field," *J. Magn. Reson.*, vol. 188, pp. 74-82, 2007.